Available online at www.sciencedirect.com
ScienceDirect
Mendeleev Commun., 2017, **27**, 150–152
Mendeleev Communications

Parallel entanglement variations in two coordination polymers derived from symmetrical and unsymmetrical V-shaped ligands

Ling Qin,*[a,b,c] Jin Li,[a] Qing-He Liu,[a] Hong-Zhe Chen,[a] Xi-Yang,[a] Fu-Hu Cao[a] and Juan Li[a]

[a] *Department of Chemical Engineering and Food Processing, Xuancheng Campus, Hefei University of Technology, Xuancheng 242000, Anhui, P. R. China. E-mail: qinling@hfut.edu.cn*
[b] *Jiangsu Engineering Technology Research Center of Environmental Cleaning Materials (CEM), School of Environmental Sciences and Engineering, Nanjing University of Information Science and Technology, Nanjing 210044, P. R. China*
[c] *State Key Laboratory of Coordination Chemistry, School of Chemistry and Chemical Engineering, Nanjing National Laboratory of Microstructures, Nanjing University, Nanjing 210093, P. R. China*

DOI: 10.1016/j.mencom.2017.03.014

Two new coordination compounds with various parallel interpenetration forms {[Cd(L1)(sdb)·H_2O]}$_n$ and {[Zn(L2)(hfipbb)]·H_2O}$_n$ {L1 = *N,N′*-bis(4-pyridyl)isophthalamide, L2 = 4,4′-([1,1′:4′,1′′-terphenyl]-3,4′′-diyl)dipyridine, H_2hfipbb = 4,4′-(hexafluoroisopropylidene) bis(benzoic acid), 4,4′-sdb = 4,4′-sulfonyl dibenzoate} have been synthesized based on two V-shaped pyridine ligands, that is, symmetrical L1 and unsymmetrical L2 ones. The compounds were characterized by elemental analyses and single crystal X-ray diffraction studies.

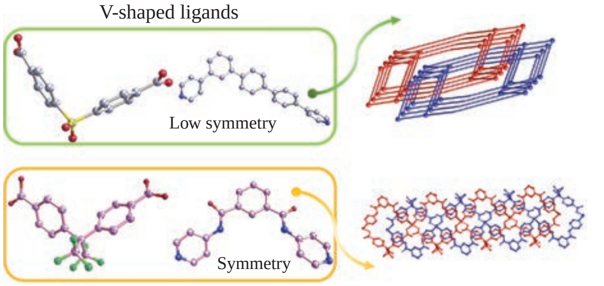

Coordination polymers (CPs) with entangled structures have been intensively studied because of their intrinsic aesthetic appeal, topological features and potential applications.[1–7] The particularly interesting discovery of coordination polymers with novel modes of supramolecular entanglements contributes to our knowledge of self-assembly processes. The entanglements mainly conclude helices, interpenetrations, polycatenations, catenanes, rotaxanes, knots and other non-typical entangled structures.[8–16] The modulation of the entangled structures, which is more closely related to the coordination mode of metal nodes, metal-to-ligand ratios, temperature, pH, solvents and the backbones of organic ligands, is still a significant challenge.[17–20]

Much effort has been devoted to the design of entangled polymers through the self-assembly of V-shaped organic acids and metal cations.[21–23] In addition, the employment of long ligands usually generates entangled frameworks. Matzger *et al.*[24,25] proposed a strategy to construct CPs using reduced symmetrical ligands. Herein, we report a systematic exploration of the V-shaped backbones of organic pyridine ligands with different symmetry and V-shaped carboxylic acid ligands. Then, we got two parallel entanglement coordination polymers, {[Cd(L1)(sdb)]·H_2O}$_n$ **1**, {[Zn(L2)(hfipbb)]·H_2O}$_n$ **2** and the details of their syntheses,[†] and structures.[‡] Compound **1** consists of the parallel interpenetration of 2D layers with left-handed and right-handed helices simultaneously. Each layer is achiral, and it further intersperses with the adjacent layers, leading to a 2D network ($2D_{achiral}/2D_{achiral} \rightarrow 2D_{achiral}$), while compound **2** is an uncommon example of $2D_{chiral}/2D_{chiral} \rightarrow 2D_{achiral}$ networks.

The X-ray crystallographic analysis has revealed that complex **1** crystallizes in the monoclinic space group $P2_1/n$. The asymmetric unit of **1** consists of one Cd^{II} cation, one L1 ligand, one 4,4′-sdb ligand and a coordinated water molecule. As shown in Figure 1(*a*), each Cd(1) cation is seven-coordinated with a pentagonal bipyramid geometry, which is formed by five oxygen atoms from two bidentate chelating carboxyl groups and one

---

[†] Commercial reagents and solvents of reagent grade were used as received. The ligands L1 and L2 were prepared by published methods.[26–28]

General procedure for the preparation of {[Cd(L1)(sdb)]·H_2O}$_n$ **1**. A mixture of $Cd(NO_3)_2 \cdot 4H_2O$ (30.8 mg, 0.1 mmol), L1 (31.8 mg, 0.1 mmol), and 4,4′-H_2sdb (30.6 mg, 0.1 mmol) was dissolved in 6 ml of distilled water and 3 ml of DMF. The final mixture was sealed in a 15 ml Parr Teflon-lined stainless-steel vessel and heated at 95 °C for three days and then cooled to room temperature. Colorless block crystals of **1** obtained were washed with water and dried under ambient conditions. Yield 43% for **1** based on L1. Found (%): C, 61.62; H, 3.66; N, 3.37. Calc. for $C_{42}H_{30}CdN_2O_7S$ (%): C, 61.58; H, 3.69; N, 3.41.

Synthesis of {[Zn(L2)(hfipbb)]·H_2O}$_n$ **2**. A mixture of $Zn(NO_3)_2 \cdot 6H_2O$ (29.7 mg, 0.1 mmol), L2 (38.4 mg, 0.1 mmol), and 4,4′-H_2hfipbb (39.2 mg, 0.1 mmol) was dissolved in 3 ml of distilled water and 3 ml of DMF. The final mixture was sealed in a 15 ml Parr Teflon-lined stainless-steel vessel and heated at 95 °C for three days and then cooled to room temperature. Colorless block crystals of **2** obtained were washed with water and dried under ambient conditions. Yield 36% for **2** based on L2. Found (%): C, 53.11; H, 3.08; N, 7.01. Calc. for $C_{35}H_{22}F_6N_4O_6Zn \cdot H_2O$ (%): C, 53.08; H, 3.05; N, 7.04.

[‡] *Crystallographic data for* **1**. $C_{42}H_{30}CdN_2O_7S$, $M = 819.14$, monoclinic, space group $P2_1/n$, $a = 6.6448(11)$, $b = 21.084(3)$ and $c = 25.500(4)$ Å, $\beta = 92.491(3)°$, $V = 3569.2(10)$ Å^3, $Z = 4$, $d_{calc} = 1.524$ g cm^{-3}, μ(MoKα) = 0.726 mm^{-1}, $F(000) = 1664$, $T = 296(2)$ K, 19560 reflections measured, 3859 independent reflections ($R_{int} = 0.1215$), final $R_1 = 0.0791$ [$I > 2\sigma(I)$], $wR(F^2) = 0.2013$, GOF = 1.004.

Crystallographic data for **2**: $C_{35}H_{22}F_6N_4O_6Zn$, $M = 773.94$, triclinic, space group $P\bar{1}$, $a = 12.2101(19)$, $b = 12.808(2)$ and $c = 14.495(2)$ Å, $\alpha = 111.050(3)°$, $\beta = 93.224(3)°$, $\gamma = 102.741(3)°$, $V = 2040.5(5)$ Å^3, $Z = 2$, $d_{calc} = 1.260$ g cm^{-3}, μ(MoKα) = 0.672 mm^{-1}, $F(000) = 784$, $T = 296(2)$ K, 14968 reflections measured, 3982 independent reflections ($R_{int} = 0.0968$), final $R_1 = 0.0778$ [$I > 2\sigma(I)$], $wR_2 = 0.1927$, GOF = 0.838.

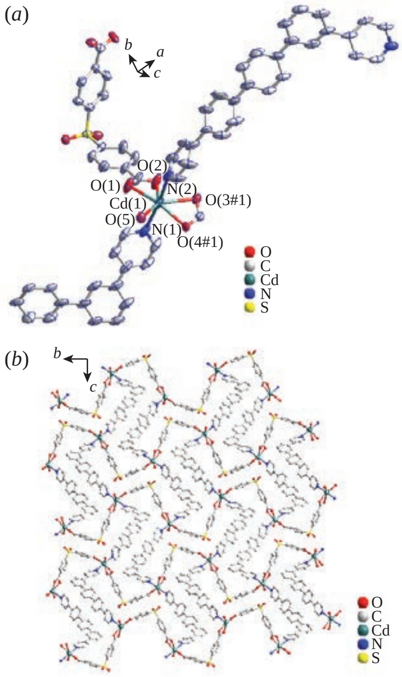

Figure 1 (*a*) Coordination environment of the Cd^{2+} cation in **1**. The hydrogen atoms are omitted for clarity. Symmetry code: #1 = $2.5 - x$, $-0.5 + y$, $1.5 - z$. (*b*) Schematic representation of a single 2D layer formed by Cd^{2+}, L1 and sdb^{2-} of compound **1**.

water molecule in the equatorial plane, and two nitrogen atoms from two L1 ligands in the perpendicular plane. The Cd cations are connected by 4,4′-sdb ligands to give a 1D structure, which are further connected by L1 ligands to generate a 2D framework [Figure 1(*b*)]. It is obvious that the mixed ligands in a V-shaped configuration connected adjacent Cd atoms to form 1D left-handed and right-handed helices with a long pitch of 21.084 Å, which are labeled as green and red cylinders in Figure 2(*a*). However, the left and right single meso-helices are coexisting and arranged alternatively in the crystal structure, the whole crystal is racemic and does not exhibit chirality. It is interesting that there is a large ring-like structure in each layer, which permits the same ring from the adjacent layer to interlock. The two layers are penetrated by each other in a parallel mode, and compound **1** shows an overall 2D$_{\text{achiral}}$ + 2D$_{\text{achiral}}$ → 2D$_{\text{achiral}}$ intercatenated framework [Figure 2(*b*)].

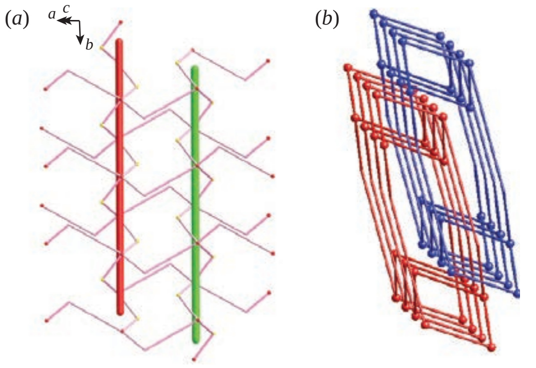

Figure 2 (*a*) View of 2D layer **1** with meso-helical chains (the green and red pillars represent the left-handed and right-handed helical chains, respectively). (*b*) Schematic view of two layers penetrated by each other in a parallel mode into a polycatenation net.

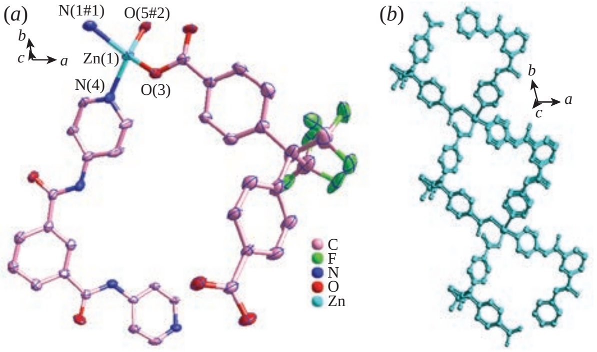

Figure 3 (*a*) Coordination environments of complex **2** (30% ellipsoid probability). Most hydrogen atoms and solvent water molecules are omitted for clarity. Symmetry codes for **2**: #1 = x, $1 + y$, $1 + z$; #2 = x, $1 + y$, z. (*b*) View of a single 2D layer formed by Zn^{2+}, L2 and hfipbb^{2-} of compound **2**.

The X-ray single-crystal structural analysis has shown that complex **2** is a 2D layer crystallized in the triclinic $P\bar{1}$ space group. The asymmetric unit contains two independent Zn$^{\text{II}}$ centers, one deprotonated hfipbb^{2-} anion, one L2 molecule and one squeezed water molecule [Figure 3(*a*)]. Zn(1) exhibits tetrahedral geometry, which is four-coordinated and formed by two O atoms [O(3), O(5)] from two monodentate hfipbb^{2-} ligands, and two N atoms [N(1), N(4)] from two L2 ligands, [Zn(1)–O 2.378(3)–2.441(3) Å, Zn(1)–N 2.341(3)–2.424(3) Å]. In **2**, the L2 ligands coordinate to Zn(1) ions to form 1D chains, which are connected by the hfipbb^{2-} ligand to result in a 2D layer [Figure 3(*b*)]. In complex **2**, in the absence of guest molecules to fill the large void space in the 2D sheets, each layer in the offset ABAB manners parallel interpenetrates forming a 2D → 2D parallel type. Unlike **1**, it contains the 2D meso-helical sheet consisting of alternant left-handed and right-handed helical chains, the racemic complex, which consists of separate left- and right-handed helical chains in different layers in compound **2** [Figure 4(*a*)]: one sheet is left-handed while the other is right-handed, is not common (2D$_{\text{chiral}}$/2D$_{\text{chiral}}$ → 2D$_{\text{achiral}}$).[32,33] The 2D meso-helical inter-

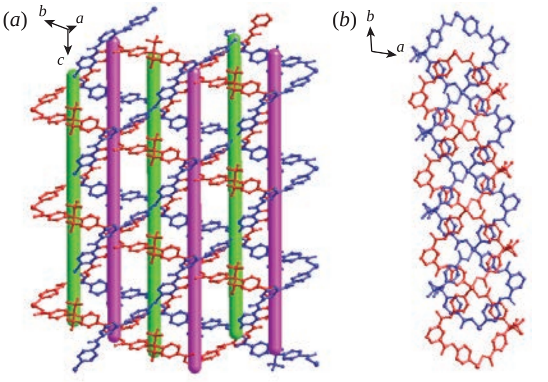

Figure 4 (*a*) View of 2D$_{\text{chiral}}$ + 2D$_{\text{chiral}}$ → 2D$_{\text{achiral}}$ stacked sheet constructed by two identical 2D layers (the green and red pillars represent left-handed and right-handed helices, respectively). (*b*) Schematic view of the entanglemental structure along the *c* axis.

The measurements were made on a Bruker Apex Smart CCD diffractometer with graphite-monochromated MoKα radiation (λ = 0.71073 Å). The structure was solved by direct methods, and the non-hydrogen atoms were located from the trial structure and then refined anisotropically with SHELXTL using full-matrix least-squares procedures based on F^2 values.[29] The distributions of peaks in the channels of **2** were chemically featureless to refine using conventional discrete-atom models. To resolve these issues, the contribution of the electron density by the remaining water molecule was removed by the SQUEEZE routine in PLATON.[30] Hydrogen atoms positions were fixed geometrically at calculated distances and allowed to ride on the parent atoms. A semiempirical absorption correction was applied using SADABS.[31]

CCDC 1482602 and 1482603 contain the supplementary crystallographic data for this paper. These data can be obtained free of charge from The Cambridge Crystallographic Data Centre *via* http://www.ccdc.cam.ac.uk.

penetrating layer contains alternant left-handed and right-handed helical chains with a pitch of 14.495 Å. The interpenetrated motif is 2-crossing [2]-catenane [Figure 4(*b*)].

The configurations of V-shaped molecules can be assessed by comparing the distortion angles defined by the coordination metal atoms and central atoms of ligands (A). In compound **1**, the angles of A for L1 are 110.70(5)°; the angles of A for sdb^{2-} are 95.47(16)° (Figure S1, see Online Supplementary Materials). In compound **2**, the angles of A for L2 are 102.94(6)°; the angles of A for hfipbb^{2-} are 99.86(99)°.

In summary, we have synthesized two new coordination polymers $\{[\mathrm{Cd(L1)(sdb)}]\cdot\mathrm{H_2O}\}_n$ **1** and $\{[\mathrm{Zn(L2)(hfipbb)}]\cdot\mathrm{H_2O}\}_n$ **2** based on two V-shaped symmetrical L1 and unsymmetrical L2 ligands and two V-shaped carboxylate co-ligands. They are the entangled nets of meso-helical chains, that is, right-handed and left-handed helices. Compound **1** shows an overall $2\mathrm{D_{achiral}} + 2\mathrm{D_{achiral}} \rightarrow 2\mathrm{D_{achiral}}$ intercatenated framework. In compound **2**, the 2D ABAB stack networks, in which left- and right-handed helical chains coexist and array alternately ($2\mathrm{D_{chiral}}/2\mathrm{D_{chiral}} \rightarrow 2\mathrm{D_{achiral}}$), make it an interesting member of 2D entangled networks.

This work was supported by the National Natural Science Foundation of China (grant no. 21601045), the China Postdoctoral Fund (grant no. 2016M601768), the Startup Foundation of Hefei University of Technology (grant nos. JZ2014HGBZ0358 and XC2015JZBZ05), the Fundamental Research Funds for the Central Universities (grant no. JZ2016HGTA0679), Open Fund by Jiangsu Engineering Technology Research Center of Environmental Cleaning Materials (grant no. KFK1505), and a project funded by the Priority Academic Program Development of Jiangsu Higher Education Institutions (PAPD).

Online Supplementary Materials

Supplementary data associated with this article can be found in the online version at doi:10.1016/j.mencom.2017.03.014.

References

1 F.-J. Liu, D. Sun, H.-J. Hao, R.-B. Huang and L.-S. Zheng, *CrystEngComm*, 2012, **14**, 379.
2 G.-L. Wen, Y.-Y. Wang, Y.-N. Zhang, G.-P. Yang, A.-Y. Fu and Q.-Z. Shi, *CrystEngComm*, 2009, **11**, 1519.
3 D. Singh and C. M. Nagaraja, *Cryst. Growth Des*., 2015, **15**, 3356.
4 G.-P. Yang, L. Hou, L.-F. Ma and Y.-Y. Wang, *CrystEngComm*, 2013, **15**, 2561.
5 V. N. Vukotic, C. A. O'Keefe, K. Zhu, K. J. Harris, C. To, R. W. Schurko and S. J. Loeb, *J. Am. Chem. Soc*., 2015, **137**, 9643.
6 J.-Y. Lu and A. M. Babb, *Inorg. Chem*., 2001, **40**, 3261.
7 D.-S. Li, Y.-P. Wu, J. Zhao, J. Zhang and J.-Y. Lu, *Coord. Chem. Rev.*, 2014, **261**, 1.
8 M.-D. Zhang, Y. Qiu, M.-X. Song, S. Ren, C.-Y. Huang and M.-D. Chen, *Mendeleev Commun*., 2016, **26**, 415.
9 J.-S. Hu, C.-H. Zhou, Y.-M. Wang, K.-P. Xu and Y.-W. Li, *Mendeleev Commun*., 2015, **25**, 211.
10 J.-S. Hu, L. Qin, M.-D. Zhang, X.-Q. Yao, Y.-Z. Li, Z.-J. Guo, H.-G. Zheng and Z.-L. Xue, *Chem. Commun.*, 2012, **48**, 681.
11 Z.-G. Kong, S.-N. Guo, X.-Y. Zhao and X. An, *Mendeleev Commun.*, 2016, **26**, 52.
12 T.-T. Wei, H. Xie, H.-C. Ma, Z.-Q. Lei, J.-C. Liu and X.-Q. Yao, *Mendeleev Commun*., 2016, **26**, 341.
13 L. Carlucci, G. Ciani and D. M. Proserpio, *Coord. Chem. Rev*., 2003, **246**, 247.
14 L. Qin, C. Mei, W.-J. Zuo, Y.-G. Wu, R.-Y. Yan and Y.-Q. Wang, *Mendeleev Commun*., 2016, **26**, 449.
15 L. Qin, M. Zhang, Q. Yang, Y. Li and H. Zheng, *Cryst. Growth Des.*, 2013, **13**, 5045.
16 M.-D. Zhang, C.-M. Di, L. Qin, X.-Q. Yao, Y.-Z. Li, Z.-J. Guo and H.-G. Zheng, *Cryst. Growth Des.*, 2012, **12**, 3957.
17 L.-W. Han, Y. Gong, Z.-J. Lin, J. Lu and R. Cao, *Dalton Trans.*, 2012, **41**, 4146.
18 F. Luo, Y.-X. Che and J.-M. Zheng, *Microporous Mesoporous Mater.*, 2009, **117**, 486.
19 M. Yang, F. Jiang, Q. Chen, Y. Zhou, R. Feng, K. Xiong and M. Hong, *CrystEngComm*, 2011, **13**, 3971.
20 S. Wang, L. Li, J. Zhang, X. Yuan and C.-Y. Su, *J. Mater. Chem.*, 2011, **21**, 7098.
21 J.-Q. Liu, Y.-Y. Wang and Y.-S. Huang, *CrystEngComm*, 2011, **13**, 3733.
22 J.-C. Jin, Y.-Y. Wang, P. Liu, R.-T. Liu, C. Ren and Q.-Z. Shi, *Cryst. Growth Des*., 2010, **10**, 2029.
23 L. Qin, J.-S. Hu, Y.-Z. Li and H.-G. Zheng, *Cryst. Growth Des.*, 2012, **12**, 403.
24 J. K. Schnobrich, O. Lebel, K. A. Cychosz, A. Dailly, A. G. Wong-Foy and A. J. Matzger, *J. Am. Chem. Soc*., 2010, **132**, 13941.
25 L. Qin, J.-S. Hu, Y.-Z. Li and H.-G. Zheng, *Cryst. Growth Des*., 2011, **11**, 3115.
26 N. N. Adarsh, D. K. Kumar and P. Dastidar, *CrystEngComm*, 2009, **11**, 796.
27 Y. Gong, Y. Zhou, J. Li, R. Cao, J. Qin and J. Li, *Dalton Trans.*, 2010, **39**, 9923.
28 O. Ohmori, M. Kawano and M. Fujita, *CrystEngComm*, 2004, **6**, 51.
29 G. M. Sheldrick, *Acta. Crystallogr., Sect. A*, 2008, **64**, 112.
30 A. L. Spek, *Acta Crystallogr., Sect. A*, 1990, **46**, 194.
31 *Bruker, APEX2, SAINT and SADABS*, Bruker AXS Inc., Madison, Wisconsin, USA, 2005.
32 J.-S. Hu, X. Zhuo, X.-H. Liu, H.-L. Xing, J. He and H.-G. Zheng, *Inorg. Chem. Commun.*, 2013, **33**, 15.
33 B. Mu, F. Li and K. S. Walton, *Chem. Commun.*, 2009, **45**, 2493.

Received: 7th July 2016; Com. 16/4986